Mobile impurity probing a two-dimensional superfluid phase transition

R. Alhyder [1,*] and G. M. Bruun [1,2]

[1] Center for Complex Quantum Systems, Department of Physics and Astronomy, Aarhus University, Ny Munkegade 120, DK-8000 Aarhus C, Denmark

[2] Shenzhen Institute for Quantum Science and Engineering and Department of Physics, Southern University of Science and Technology, Shenzhen 518055, China

(Received 28 December 2021; revised 3 March 2022; accepted 16 May 2022; published 3 June 2022)

The use of atomically sized quantum systems as highly sensitive measuring devices represents an exciting and quickly growing research field. Here we explore the properties of a quasiparticle formed by a mobile impurity interacting with a two-dimensional fermionic superfluid. The energy of the quasiparticle is shown to be lowered by superfluid pairing, as this increases the compressibility of the Fermi gas, thereby making it easier for the impurity to perturb its surroundings. We demonstrate that the fundamentally discontinuous nature of the superfluid-to-normal phase transition of a two-dimensional system leads to a rapid increase in the quasiparticle energy around the critical temperature. The magnitude of this increase exhibits a nonmonotonic behavior as a function of the pairing strength with a sizable maximum in the crossover region, where the spatial extend of the Cooper pairs is comparable to the interparticle spacing. Since the quasiparticle energy is measurable with present experimental techniques, our results illustrate how impurities entangled with their environment can serve as useful probes for nontrivial thermal and quantum correlations.

DOI: 10.1103/PhysRevA.105.063303

I. INTRODUCTION

The realization of accurate measuring devices, which are based on their quantum-mechanical properties, represents a new and exciting research direction with great technological potential. A main goal is to develop atomically sized probes with maximal sensitivity and minimal back action on the environment [1]. Impurity atoms are promising candidates for this, and they have already been used experimentally to measure the temperature [2–4] and density [5] of a surrounding quantum degenerate gas, as well as to detect induced interactions [6]. So far, the vast majority of investigations into mobile impurities in atomic gases concerned cases where the environment is either a weakly interacting Bose-Einstein condensate (BEC) or an ideal Fermi gas, and the impurity forms a quasiparticle called the Bose or Fermi polaron, respectively [7–15].

Much less attention has been payed to mobile impurities in environments with correlations between the particles. The properties of an impurity in a fermionic superfluid across the strongly correlated BCS-BEC crossover were examined [16,17], but a general description turns out to be complicated by the presence of ultraviolet divergencies related to three-body physics [18]. A particularly interesting case concerns two-dimensional (2D) systems, where quantum and thermal fluctuations are more pronounced than in 3D and true long-range order is prohibited at a nonzero temperature [19,20]. Nevertheless, 2D systems can exhibit a so-called Berezinskii-Kosterlitz-Thouless (BKT) phase transition to a superfluid phase with quasi-long-range order [21–23], which has been observed in a range of bosonic systems including ^{4}He films [24], magnetic layers [25], and atomic Bose gases [26–30]. A 2D superfluid in a two-component, strongly interacting atomic Fermi gas was observed only recently [31–33], and the underlying discontinuity of the phase transition has so far not been seen unambiguously in this system. In general, our understanding of 2D fermionic superfluids is less developed as compared to their bosonic counterparts.

Here we investigate a mobile impurity immersed in a 2D fermionic superfluid. Interactions between the impurity and the surrounding fermions lead to the formation of a quasiparticle, i.e., a polaron, and we show that its energy is lowered due to an increase in the compressibility of the environment caused by superfluid pairing. We furthermore demonstrate that the abrupt vanishing of the superfluid density at the critical temperature, characteristic for a superfluid-to-normal phase transition in 2D [34], gives rise to a rapid increase in the polaron energy. The increase depends nonmonotonically on the Fermi-Fermi interaction strength, exhibiting a maximum when the size of the Cooper pairs is comparable to the interparticle spacing. Our results show how a mobile impurity can serve as a sensitive probe for thermal and quantum correlations of a 2D fermionic system, thereby providing important guides for improving our understanding of its nontrivial superfluid-to-normal phase transition.

II. SYSTEM

Consider an impurity of mass m_I immersed in a two-component ($\sigma = \uparrow, \downarrow$) gas of fermions of mass m in 2D. The $\uparrow$ and $\downarrow$ fermions interact attractively and form a superfluid below a critical temperature. Using BCS theory to describe

*Corresponding author: ragheed.alhyder@phys.au.dk

this superfluid phase, the Hamiltonian of the system is

$$\hat{H} = \sum_{k\sigma} \xi_k \hat{a}^\dagger_{k\sigma} \hat{a}_{k\sigma} + \Delta \sum_{k} (\hat{a}_{-k\downarrow}\hat{a}_{k\uparrow} + \hat{a}^\dagger_{-k\uparrow}\hat{a}^\dagger_{k\downarrow}) + \sum_{k} \epsilon_k \hat{c}^\dagger_k \hat{c}_k + g_{\rm IF} \sum_{kk'q\sigma} \hat{a}^\dagger_{k'-q\sigma}\hat{a}_{k'\sigma}\hat{c}^\dagger_{k+q}\hat{c}_k. \tag{1}$$

Here, $\hat{a}^\dagger_{k\sigma}$ is the creation operator of a fermion with momentum $\boldsymbol{k}$, spin σ, and kinetic energy $\xi_k = k^2/2m - \mu$, with μ the chemical potential, and $\hat{c}_k$ creates an impurity with momentum $\boldsymbol{k}$ and kinetic energy $\epsilon_k = k^2/2m_I$. $g_{\rm IF}$ is the interaction strength for momenta less than a cutoff Λ, which can be eliminated in favor of a two-body bound state with energy ϵ_B using [35,36]

$$\frac{1}{g_{\rm IF}} = -\frac{1}{\mathcal{V}} \sum_{|q|<\Lambda} \frac{1}{E_B + q^2/2m_r}, \tag{2}$$

where $m_r = mm_i/(m+m_i)$ and $E_B = 1/2m_r a^2_{IF}$.

The superfluid gap Δ at temperature T is determined from

$$\Delta = -\frac{g_{\rm F}}{\beta\mathcal{V}} \sum_{k,n} G_{12}(\boldsymbol{k}, i\omega_n), \tag{3}$$

where G_{12} is the anomalous Green's function. This leads to the following gap equation:

$$\int dk\, k\left(\frac{\tanh(E_k/2T)}{2E_k} - \frac{1}{\epsilon_B + k^2/2m_r}\right) = 0, \tag{4}$$

where $E_k = \sqrt{\xi^2_k + \Delta^2}$, and we have renormalized the gap equation by replacing the Fermi-Fermi interaction strength by the energy of a bound state of two fermions ϵ_B, which is always present for an attractive interaction [35]. We work in units where $\hbar$, k_B, and the system volume are all unity.

III. THE BKT TRANSITION

The 2D superfluid with quasi-long-range order melts into a normal phase when vortex and antivortex pairs unbind and proliferate. This occurs at the critical temperature determined by the condition [22,37]

$$T_{\rm BKT} = \frac{\pi}{8m} n_s(T_{\rm BKT}), \tag{5}$$

where n_s is the superfluid density given by [38]

$$\frac{n_s(T)}{n} = 1 + \frac{1}{2\pi mn}\int_0^\infty dk k^3 \frac{\partial f(E_k)}{\partial E_k}. \tag{6}$$

Here $f(E) = [\exp(E/T)+1]^{-1}$ is the Fermi-Dirac distribution, and $n = k_F^2/2\pi$ is the total density from both spin states of the Fermi gas. The integral is always negative and vanishes at $T = 0$, ensuring that the superfluid density is always equal to or smaller than the total density. It follows from Eq. (5) that the superfluid density of the Fermi gas exhibits a universal jump $\Delta n_s/mT_{\rm BKT} = 8/\pi$ at the BKT transition. This jump has not yet been observed in the experiments exploring two-dimensional atomic Fermi gases, and a main goal here is to demonstrate that the discontinuity of the phase transition can be detected by looking at the properties of the impurity.

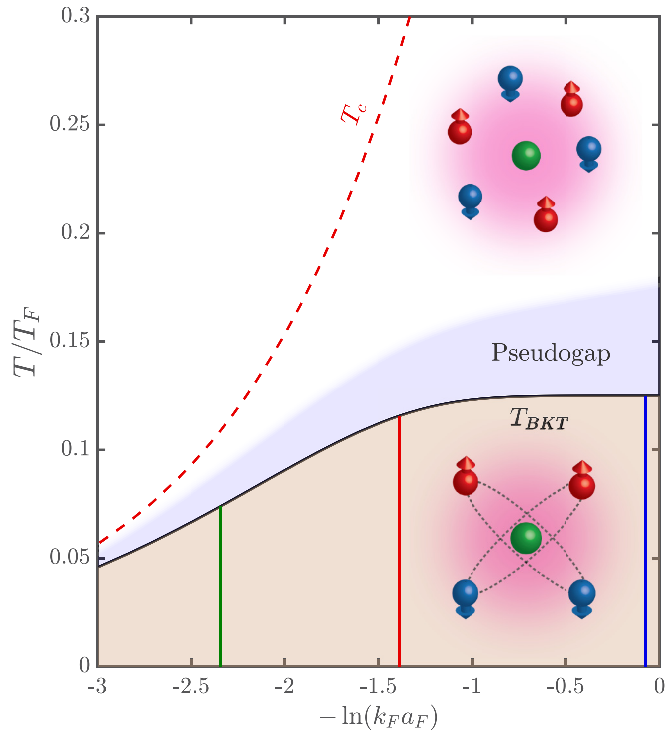

FIG. 1. We consider a mobile impurity (green ball without arrow) forming a quasiparticle by interacting with a two-component Fermi gas (blue and red balls with arrows) in 2D. An attractive interaction with strength $-\ln(k_F a_F)$ between the fermions gives rise to a discontinuous phase transition between a superfluid and a normal phase at the critical temperature $T_{\rm BKT}$, which is suppressed from the mean-field BCS prediction T_c by phase fluctuations. The vertical lines indicate the coupling strengths for which we plot the polaron energy in Fig. 2.

Figure 1 shows the phase diagram of the Fermi gas as a function of the Fermi-Fermi interaction length strength parametrized by $-\ln(k_F a_F)$ and temperature. Here, a_F is a scattering length defined by writing the energy of the bound Fermi-Fermi dimer as $-1/ma^2_F$. The Fermi gas is in a superfluid phase below a critical temperature $T_{\rm BKT}$ obtained by solving Eqs. (4)–(6) self-consistently. We vary the chemical potential μ to keep the density $n = 2\sum_{\mathbf{k}}[v^2_{\mathbf{k}}(1-f_{\mathbf{k}}) + u^2_{\mathbf{k}} f_{\mathbf{k}}]$ fixed, where $v^2_{\boldsymbol{k}} = 1 - u^2_{\boldsymbol{k}} = (1 - \xi_{\boldsymbol{k}}/E_{\boldsymbol{k}})/2$ are the coherence factors.

For weak coupling $-\ln(k_F a_F) \ll -1$, corresponding to the so-called BCS regime with large Cooper pairs, the superfluid transition temperature is close to that obtained from mean-field BCS theory, which predicts a smooth decrease of the superfluid density to zero at the critical temperature T_c. It follows that the jump in the superfluid density at $T_{\rm BKT}$ is small for weak coupling. For stronger coupling, however, phase fluctuations significantly suppress the critical temperature below the BCS prediction, leading to a large jump in the superfluid density at the phase transition. We obtain $T_{\rm BKT} = T_F/8$ in the strong-coupling regime with $-\ln(k_F a_F) \gtrsim -1$, reflecting that the superfluid density equals the total density $n = k_F^2/2\pi$ just below the transition, giving rise to a maximal jump $\Delta n_s = n$ [39–41]. We note, however, that the gas eventually enters the BEC regime with increasing $-\ln(k_F a_F) \gtrsim 1$, where it can be described as a Bose gas of tightly bound Cooper pairs with a BKT critical temperature that decreases slowly [31,32,42,43].

IV. PERTURBATION THEORY

We now turn to the properties of the impurity in the Fermi gas. Since the case of general interaction strengths between the impurity and the fermions as well as between the fermions is very complicated, we focus on the regime of weak impurity-fermion interactions where a reliable perturbative theory can be developed.

To do this, consider the scattering matrix between the impurity and a fermion. As detailed in Appendix A, it can in the ladder approximation be written as

$$\mathcal{T}(k) = \frac{g}{1 - g\Delta\Pi(k)} \simeq g + g^2\Delta\Pi(k) + \cdots, \tag{7}$$

where $k = (\boldsymbol{k}, i\omega_n)$ denotes the center-of-mass momentum $\boldsymbol{k}$ of the colliding pair with $i\omega_n$ a Matsubara frequency, and an expression for the pair propagator $\Delta\Pi(k)$ is given in Appendix B. It follows from Eq. (7) that

$$g = -\frac{\pi}{m_r}\frac{1}{\ln(k_F a_{\rm IF})} \tag{8}$$

is an effective 2D interaction strength between the impurity and the fermions [44,45]. We have thus eliminated the bare impurity-Fermi coupling strength $g_{\rm IF}$ in favor of an effective interaction strength, which is a function of the energy $-1/2m_r a_{\rm IF}^2$ of the bound impurity-fermion dimer with $a_{\rm IF}$ the impurity-fermion scattering length and $m_r = mm_I/(m + m_I)$ the reduced mass [35,36]. When $|\ln(k_F a_{\rm IF})| \gg 1$, the effective interaction is weak and the impurity properties can be calculated reliably using perturbation theory in g as used in Eq. (7).

To first order in g, the energy shift of the impurity is simply given by the mean-field expression $\Sigma_1(p) = gn$. The second-order term is

$$\Sigma_2(p) = 2Tg^2\sum_k [G_{11}(k)\Delta\Pi(p+k) + G_{12}(k)\Pi_{21}(p+k)]$$
$$= Tg^2\sum_k G_0(k)\chi(p-k), \tag{9}$$

where

$$G_{11}(\boldsymbol{k}, i\omega_n) = \frac{u_{\boldsymbol{k}}^2}{i\omega_n - E_{\boldsymbol{k}}} + \frac{v_{\boldsymbol{k}}^2}{i\omega_n + E_{\boldsymbol{k}}}, \tag{10}$$

$$G_{12}(\boldsymbol{k}, i\omega_n) = u_{\boldsymbol{k}}v_{\boldsymbol{k}}\left(\frac{1}{i\omega_n + E_{\boldsymbol{k}}} - \frac{1}{i\omega_n - E_{\boldsymbol{k}}}\right) \tag{11}$$

are the normal and anomalous propagators for the superfluid, and $G_0^{-1}(k) = i\omega_n - \epsilon_k$ is the impurity Green's function in the absence of interactions. The first term in the first line of Eq. (9) describes the coupling of the impurity to particle-hole excitations in the superfluid, whereas the second term describes coupling to pair-breaking excitations. In the second line of Eq. (9), we write the impurity self-energy in terms of the density-density correlation function $\chi(k)$ of the superfluid, which gives the compressibility for long wave lengths. Expressions for $\Pi_{12}(k)$ and $\chi(k)$ are given in Appendix B.

The energy ϵ_P of the polaron can now be found from the pole of the impurity Green's function $G(k)$ analytically continued to real frequencies. Using the Dyson equation $G^{-1}(k) = G_0^{-1}(k) - \Sigma(k)$ with $\Sigma(k) = \Sigma_1(k) + \Sigma_2(k)$ to second order in g then yields

$$\epsilon_P = gn + \Sigma_2(0, \epsilon_P + i0_+), \tag{12}$$

where we take zero momentum and $m_I = m$ in the following for simplicity.

V. NORMAL PHASE

Strictly speaking, it is only the superfluid density that exhibits a discontinuity at T_{BKT}. This is because the long-range phase coherence of the gap is lost for $T > T_{BKT}$, whereas its amplitude $|\Delta|$ remains continuous. In the following we will nevertheless assume that the pairing gap jumps to zero at the temperature T_{BKT} for the BKT phase transition. That is, we will use BCS theory for $T \leqslant T_{BKT}$ and set $\Delta = 0$ for $T > T_{BKT}$, which corresponds to assuming that the Fermi gas is noninteracting. The reasons for this are the following. First, vortices with a vanishing gap in their centers proliferate at the transition temperature, which will significantly decrease the average gap for $T > T_{BKT}$. Second, even if the gap is nonzero in the normal phase, it does not lead to a perfect vanishing of the density of states around the Fermi level as opposed to in the superfluid phase. Indeed, the gap in the normal phase is often refereed to as a pseudogap for this reason, and its description requires inclusion of fluctuation effects beyond BCS theory. A central feature of the theories for the pseudogap region is that they predict a suppressed but *nonzero* density of states at the Fermi level [46,47]. This means that impurity can scatter on low-energy excitations in the surrounding bath, even for a nonzero pseudogap in the normal phase above T_{BKT}. Using a nonzero Δ in the BCS Green's functions, Eq. (11) above $T > T_{BKT}$ would, on the other hand, yield a vanishing density of states at the Fermi level, thereby missing these low-energy excitations completely, which likely will result in an unphysical polaron energy. Finally, BCS theory drastically overestimates the temperature for which the amplitude of the gap vanishes except for weak coupling. Indeed, more sophisticated theories predict that the pseudogap vanishes for temperatures much lower than the mean-field critical temperature [46,48]. It follows that the pseudogap goes to zero in a temperature range above T_{BKT} that is narrow compared to the BCS transition temperature. Given these facts, it is physically reasonable as a first approximation to assume that the gap jumps to zero at T_{BKT}, which should therefore be understood as the limiting form of a continuous but sharp drop. We therefore take $\Delta = 0$ for $T > T_{BKT}$ in the rest of the paper, which corresponds to assuming that the Fermi gas is ideal in the normal phase.

VI. RESULTS

In Fig. 2 we plot the polaron energy as a function of the temperature for different values of the Fermi-Fermi interaction, which are shown by vertical lines in Fig. 1. This is found by first solving Eqs. (4)–(6) numerically for constant density to find the properties of the Fermi bath. We then calculate

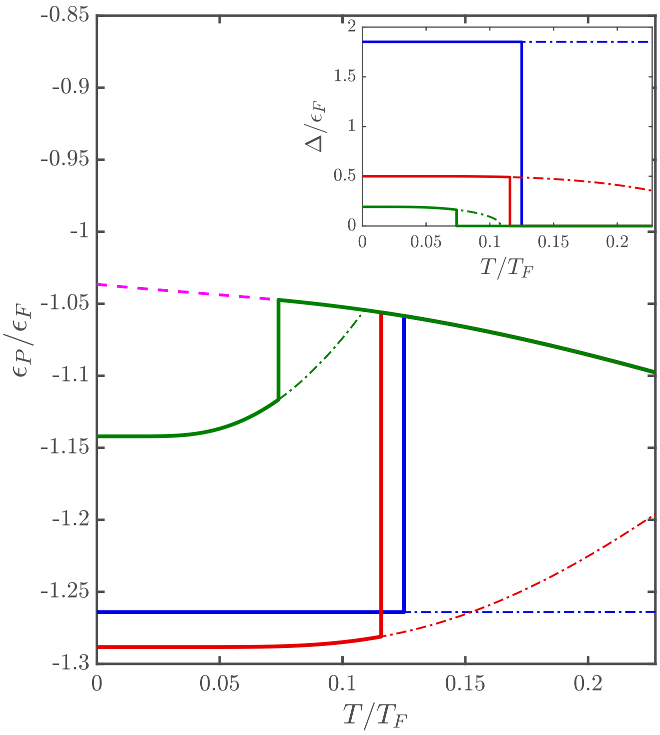

FIG. 2. Polaron energy as a function of temperature for the Fermi-Fermi coupling strengths $-\ln(k_Fa_F) = -2.342$ (green upper line), $-\ln(k_Fa_F) = -1.386$ (red lower line), and $-\ln(k_Fa_F) = -0.077$ (blue middle line). The dashed pink line gives polaron energy in the normal phase, and the dash-dotted lines the polaron energy assuming the Fermi gas remains superfluid up to the mean-field critical temperature T_c. The inset shows the superfluid gap as a function of temperature for the same coupling strengths, with the dash-dotted lines giving the mean-field prediction for $T > T_{\rm BKT}$. The colors blue (upper), red (middle), and green (lower) correspond to the scattering values of the main plot. The dotted lines illustrate the expected continuous behavior of the polaron energy and magnitude $|\Delta|$ of the gap around the BKT transition, as explained in Sec. V.

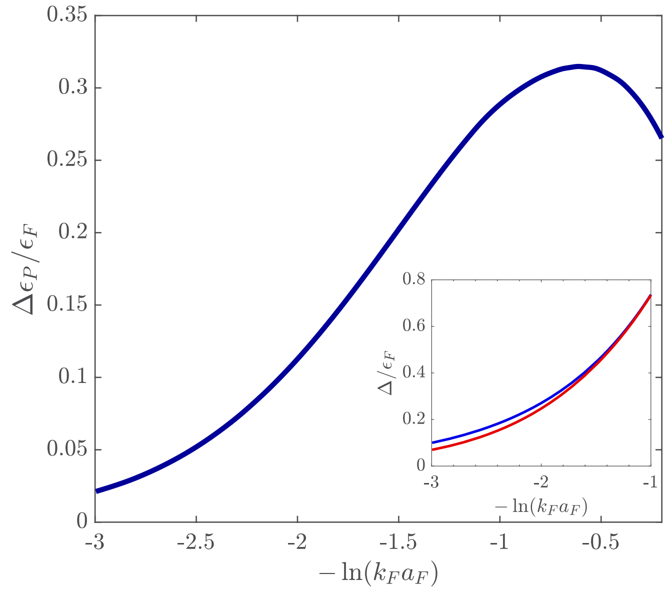

FIG. 3. The limiting discontinuity $\Delta\epsilon_P$ in the polaron energy at the critical temperature $T_{\rm BKT}$ as a function of the Fermi-Fermi coupling strength $-\ln(k_Fa_F)$. The inset shows the superfluid gap at $T = 0$ (blue upper line) and at $T = T_{\rm BKT}$ (red lower line) as a function of the interaction strength.

the impurity self-energy from Eq. (9). The impurity-fermion interaction is $-\ln(k_Fa_{\rm IF}) = -1.03$, for which perturbation theory is still accurate for an impurity in a 2D ideal Fermi gas [49]. First, we note that the polaron has a lower energy when the Fermi gas is in the superfluid phase as compared to when it is in the normal phase (dashed lines). Physically, this is because pairing correlations increase the compressibility of the Fermi gas [50–53] so that the impurity more easily can perturb its surroundings, thereby lowering the energy. As the temperature increases, the superfluid gap decreases (inset in Fig. 2) and the polaron energy approaches the value in the normal phase, which in turn decreases with temperature, in analogy with what is found in 3D [54,55]. In particular, the polaron energy exhibits a discontinuity at the critical temperature $T_{\rm BKT}$, since we assume that the superfluid gap in the surrounding medium jumps to zero at the transition. It is strictly only the superfluid density that is discontinuous at the transition due to the loss of phase coherence, whereas as the amplitude of the gap and therefore the polaron energy is continuous. Nevertheless, as we argued above, the gap must be expected to exhibit a steep decrease in a narrow region around $T_{\rm BKT}$. The results shown in Fig. 2 should in this sense be understood as a limiting form of a continuous but rapid increase in ϵ_P on the scale of the mean-field (BCS) transition temperature. This should be contrasted to BCS theory predicting a gap that goes to zero at a much higher transition temperature T_c (except for weak coupling), giving rise to a much more smooth behavior of polaron energy. Thus the abrupt change of the Fermi gas at $T_{\rm BKT}$ is reflected in the polaron energy, which exhibits a sizable and steep increase in its energy in a narrow temperature region. Importantly, this should be observable with the spectral resolution of current Fermi polaron experiments [11–15]. These results show that the polaron can be used as a probe of the abrupt nature of the superfluid-to-normal phase transition in a 2D fermionic superfluid. In particular, a measurement of the polaron energy and its behavior around $T_{\rm BKT}$ should provide valuable information regarding the thermal and quantum fluctuations in the critical region.

Figure 2 shows that the amplitude of the rapid energy increase is larger for $-\ln(k_Fa_F) = -1.386$ than for $-\ln(k_Fa_F) = -2.342$. This is as expected, since a stronger Fermi-Fermi coupling gives rise to a larger decrease in the superfluid gap (inset) at $T_{\rm BKT}$. The discontinuity is, however, smaller again for even stronger coupling with $-\ln(k_Fa_F) = -0.077$, even though the pairing energy is larger. To explore this further, we plot in Fig. 3 the value $\Delta\epsilon_P = \epsilon_P(T^+_{\rm BKT}) - \epsilon_P(T^-_{\rm BKT})$ as a function of the Fermi-Fermi coupling strength $-\ln(k_Fa_F)$, which corresponds to the change in the polaron energy in the limit where it occurs with infinite slope at $T_{\rm BKT}$. We see that $\Delta\epsilon_P$ initially increases with the coupling strength in the BCS regime. It reaches a sizable maximum of $\Delta\epsilon_P \simeq 0.32\epsilon_F$ in the crossover region around $\ln(k_Fa_F) \sim -0.6$, after which it decreases, as the BEC region is approached with

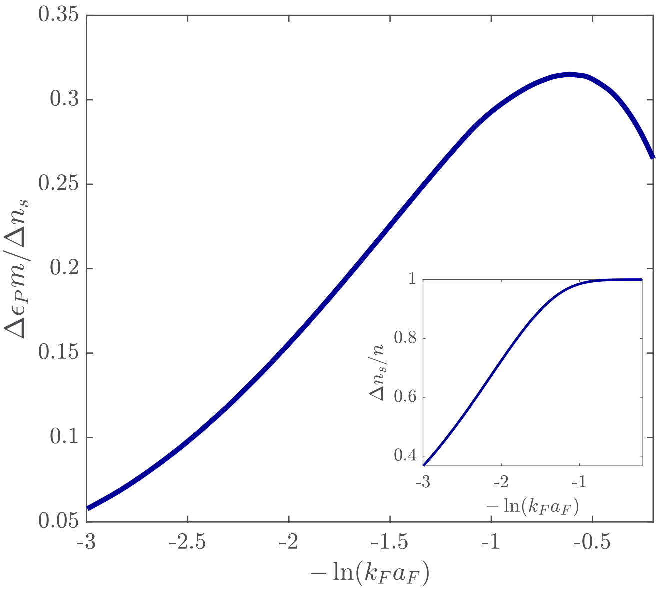

FIG. 4. The limiting discontinuity $\Delta\epsilon_P$ in the polaron energy at the critical temperature $T_{\rm BKT}$ in units of the jump Δn_s in the superfluid density as a function of the Fermi-Fermi coupling strength $-\ln(k_F a_F)$. The inset shows $\Delta n_s/n$ as a function of interaction strength.

increasing interaction, even though the gap continues to increase as shown in the inset. This should be contrasted to the gap, which increases monotonically as a function of the coupling both for $T = 0$ and $T = T_{BKT}$ as shown in the inset of Fig. 3. Interestingly, the maximum in $\Delta\epsilon_P$ occurs when the size of the Cooper pairs is comparable to the interparticle spacing, where one has also observed a maximum in the critical temperature [31,32] and in the critical velocity [33]. As the coupling strength increases further with $-\ln(k_F a_F) \gg 1$, the Cooper pairs shrink and the Fermi gas becomes a BEC of dimers with a transition temperature in a narrow region $\propto 1/\ln[\ln(1/na_D^2)]$ below the mean-field prediction, with a_D the dimer-dimer scattering length and a correspondingly small discontinuity in the superfluid density [31,32,42,43]. It follows that there *should* be a maximum in $\Delta\epsilon_P$ somewhere in the crossover region as indeed predicted here. Note, however, that our theory is unreliable in the BEC regime, since it does not include the Bogoliubov-Anderson mode, which becomes the dominant excitation compared to particle-hole and pair-breaking excitations. A consistent description of the polaron in the whole BEC-BCS crossover of the Fermi gas is remains an open and very challenging problem beyond the present scope.

Finally, Fig. 4 plots the limiting change $\Delta\epsilon_P$ in the polaron energy at T_{BKT} in units of the jump $\Delta n_s/m$ in the superfluid density at the critical temperature, which is shown in the inset. This shows that while the rapid change in the polaron energy is a direct consequence of the abrupt nature of the BKT phase transition of the surrounding medium, there is no simple proportionality between $\Delta\epsilon_P$ and Δn_s. Instead, the ratio $\Delta\epsilon_P m/\Delta n_s$ increases with Fermi-Fermi interaction strength in the BCS regime, reaching a maximum at $\ln(k_F a_F) \sim -0.6$, after which it decreases. The jump in the superfluid density at the transition temperature, on the other hand, increases monotonically with the coupling strength, reaching the limiting value n in the BEC regime.

VII. DISCUSSION AND OUTLOOK

We investigated the properties of a quasiparticle formed by a mobile impurity in a fermionic superfluid. The characteristic discontinuity of the superfluid-to-normal phase transition of a 2D system was shown to give rise to a rapid increase in the quasiparticle energy around the transition temperature. We demonstrated that the amplitude of the increase depends nonmonotonically on the pairing strength, with a maximum in the crossover region between the BCS and BEC limits, and that it is measurable with present experimental techniques. In particular, radio-frequency spectroscopy has proven to be a very powerful technique for measuring the polaron energy both in Fermi gases and in BECs [7–15].

Our results show a way to probe the properties of the superfluid as well as its transition to the normal phase for a 2D fermionic system. This is of particular interest since there is no quantitatively reliable theory for this challenging problem in the strong-coupling regime. For instance, a nonzero width of the rapid increase of the polaron energy around $T_{\rm BKT}$ will provide information regarding the pseudogap region. This could, moreover, cast light on the intriguing question regarding the role of vortex-antivortex pairs in the superfluid phase and above, and their interplay with the impurity. It would also be very interesting to develop an improved theoretical understanding regarding the properties of the BKT transition for a fermionic superfluid, including its quantum and thermal fluctuations [46,47,56,57]. Here, experimental results regarding the polaron energy in the critical region would provide important guides for this challenging problem.

The magnitude of the jump in the polaron energy will clearly be even larger for stronger interactions between the impurity and the surrounding Fermi gas. Exploring this requires going beyond the perturbative approach used here, which is an interesting topic for future study. Another fascinating but very challenging problem is to explore how the quasiparticle evolves smoothly from a Fermi to a Bose polaron as the Fermi gas changes from a BCS superfluid to a BEC of dimers.

From a broader perspective, our results illustrate how impurities entangled with their environment via particle collisions can be used as sensitive probes for nontrivial quantum and thermal correlations. This motivates further investigations into how coherent superpositions of internal spin states of the impurity can be used to enhance the sensitivity of the impurity probe while minimizing the back action on the environment [58–61]. Another intriguing research direction is to investigate how impurities can be used to probe nonlocal correlations and order, as well as the geometric and topological properties of the environment [62–66].

ACKNOWLEDGMENTS

This work has been supported by the Danish National Research Foundation through the Center of Excellence CCQ

(Grant Agreement No. DNRF156) and the Independent Research Fund Denmark – Natural Sciences via Grant No. DFF-8021-00233B.

APPENDIX A: $\mathcal{T}$ MATRIX

In order to get an expression for g_{IF} in terms of the pair propagator we write the $\mathcal{T}$ matrix in vacuum as

$$\mathcal{T}_v(\boldsymbol{k},\omega) = \frac{1}{g_{\mathrm{IF}}^{-1} - \Pi_v(\boldsymbol{k},\omega)}, \tag{A1}$$

where Π_v is the pair propagator for two fermions in a vacuum,

$$\Pi_v(\boldsymbol{k},\omega) = \frac{1}{\mathcal{V}}\sum_{\boldsymbol{q}}^{\Lambda} \frac{1}{\omega - k^2/2M - q^2/2m_r}, \tag{A2}$$

with $M = m + m_I$, and Λ is a UV cutoff that we send to infinity at the end of the calculation. We perform a variable change $q^2 = x \Rightarrow dq = dx/2\sqrt{x}$, and after a straightforward calculation we get

$$\Pi_v(\boldsymbol{k},\omega) = -\frac{m_r}{2\pi}\left[\ln\left(\left|\frac{\omega + i0_+ - k^2/2M - \Lambda}{\omega_n - k^2/2M + \mu}\right|\right) + i\pi - i\arg(\omega + i0_+ - k^2/2M)\right]. \tag{A3}$$

Lastly, since the dimer bound-state energy is a pole of the vacuum $\mathcal{T}$ matrix we can write from Eq. (A1) $g_{\mathrm{IF}}^{-1} = \Pi_v(0,\epsilon_B)$.

We can now write the scattering matrix in the medium as

$$\mathcal{T}(\boldsymbol{k}, i\omega_n) = \frac{1}{\Pi_v(0,\epsilon_B) - \Pi(\boldsymbol{k},\omega_n)}, \tag{A4}$$

where

$$\Pi(\boldsymbol{k}, i\omega_n) = \frac{1}{\mathcal{V}}\sum_{\boldsymbol{p}}\left(\frac{u_{\boldsymbol{p}}^2(1-n_{\boldsymbol{p}})}{i\omega_n - E_{\boldsymbol{p}} - \epsilon_{\boldsymbol{k}-\boldsymbol{p}}} + \frac{v_{\boldsymbol{p}}^2 n_{\boldsymbol{p}}}{i\omega_n + E_{\boldsymbol{p}} - \epsilon_{\boldsymbol{k}-\boldsymbol{p}}}\right). \tag{A5}$$

Note that here we take $\epsilon_B = -1/2m_r a_{\mathrm{IF}}^2 < 0$. In order to remove the divergence in both pair propagators, we add and subtract $\mathrm{Re}[\Pi_v(0,\epsilon_F)]$ in the denominator, and with this we can define

$$\frac{1}{g} = \Pi_v(0,\epsilon_B) - \mathrm{Re}[\Pi_v(0,\epsilon_F)] \simeq -\frac{\pi}{m_r}\frac{1}{\ln(k_F a)}, \tag{A6}$$

where we left out m_r/m since $k_F a_{\mathrm{IF}} \gg m_r/m$.

APPENDIX B: PERTURBATIVE EXPANSION

Going back to the full expression for the scattering matrix, we can expand it in the weak-coupling regime ($k_F a_{\mathrm{IF}} \gg 1$) in a perturbative series up to second order in g,

$$\mathcal{T}(\boldsymbol{k}, i\omega_n) = \frac{g}{1 - g\Delta\Pi(\boldsymbol{k}, i\omega_n)} \simeq g + g^2\Delta\Pi(\boldsymbol{k}, i\omega_n), \tag{B1}$$

where g is expressed by Eq. (A6), and

$$\Delta\Pi(\boldsymbol{k}, i\omega_n) = \Pi(\boldsymbol{k}, i\omega_n) - \mathrm{Re}[\Pi_v(0,\epsilon_F)]. \tag{B2}$$

To first order this gives the mean-field contribution to the self-energy of the polaron

$$\Sigma_1(\boldsymbol{q}, i\Omega_\nu) =$$ 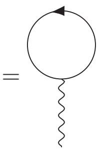 $$= 2g\sum_k G_{11}(k) \qquad (21)$$ (B3)

$\sum$ $\sum$ $\sum$

with $k = (\boldsymbol{k}, i\omega_n)$ and $\sum_k = \frac{1}{\beta\mathcal{V}}\sum_{\boldsymbol{k}}\sum_n$. After a straightforward calculation we find

$$\Sigma_1(0,\epsilon_P) = \frac{g}{\pi}\int_0^\infty dk\, k\left[u_{\boldsymbol{k}}^2 n_{\boldsymbol{k}} + v_{\boldsymbol{k}}^2(1-n_{\boldsymbol{k}})\right]. \tag{B4}$$

The second-order contribution is written in Eq. (9) of the main text with

$$\chi(k) = \sum_q [G_{11}(q)G_{11}(p-k+q) + G_{12}(q)G_{12}(p-k+q)]. \tag{B5}$$

We can write this in a different way as $\Sigma_2 = \Sigma_{2a} + \Sigma_{2b}$, where

$$\Sigma_{2a}(0,\epsilon_P) =$$ 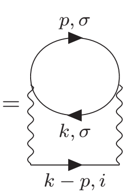

(B6)

After a straightforward calculation we find

$$\begin{aligned}\Sigma_{2a}(0,\epsilon_P) &= \frac{2g^2}{\mathcal{V}^2}\sum_{\boldsymbol{k},\boldsymbol{p}}\left(\frac{v_{\boldsymbol{p}}^2 u_{\boldsymbol{k}}^2 n_{\boldsymbol{k}} n_{\boldsymbol{p}}}{\epsilon_P + E_{\boldsymbol{k}} + E_{\boldsymbol{p}} - \epsilon_{\boldsymbol{k}-\boldsymbol{p}}}\right.\\ &+ \frac{u_{\boldsymbol{p}}^2 v_{\boldsymbol{k}}^2(1-n_{\boldsymbol{k}})(1-n_{\boldsymbol{p}})}{\epsilon_P - E_{\boldsymbol{k}} - E_{\boldsymbol{p}} - \epsilon_{\boldsymbol{k}-\boldsymbol{p}}} + \frac{v_{\boldsymbol{p}}^2 v_{\boldsymbol{k}}^2(1-n_{\boldsymbol{k}})n_{\boldsymbol{p}}}{\epsilon_P - E_{\boldsymbol{k}} + E_{\boldsymbol{p}} - \epsilon_{\boldsymbol{k}-\boldsymbol{p}}}\\ &\left.+ \frac{u_{\boldsymbol{p}}^2 u_{\boldsymbol{k}}^2 n_{\boldsymbol{k}}(1-n_{\boldsymbol{p}})}{\epsilon_P + E_{\boldsymbol{k}} - E_{\boldsymbol{p}} - \epsilon_{\boldsymbol{k}-\boldsymbol{p}}} - \frac{u_{\boldsymbol{k}}^2 n_{\boldsymbol{k}} + v_{\boldsymbol{k}}^2(1-n_{\boldsymbol{k}})}{\epsilon_F - \epsilon_F(\boldsymbol{p}) - \epsilon_I(\boldsymbol{p})}\right).\end{aligned} \tag{B7}$$

We also get

$$\Sigma_{2b}(0,\epsilon_P) =$$ 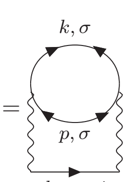

(B8)

where

$$\Pi_{21}(\boldsymbol{k}, i\omega_n + \epsilon_P) = \frac{1}{\beta\mathcal{V}}\sum_{\boldsymbol{p}}\sum_m G_{12}(\boldsymbol{p}, i\omega_m) \times G_{0,i}(\boldsymbol{k}-\boldsymbol{p}, i\omega_n - i\omega_m + \epsilon_P). \tag{B9}$$

After a straightforward calculation we can write

$$\Sigma_{2b}(0,\epsilon_P) = \frac{2g^2}{\mathcal{V}^2}\sum_{k,p} u_k v_k u_p v_p\left[\frac{n_k n_p}{\epsilon_P + E_k + E_p - \epsilon_{k-p}} + \frac{(1-n_k)(1-n_p)}{\epsilon_P - E_k - E_p - \epsilon_{k-p}} - \frac{(1-n_k)n_p}{\epsilon_P - E_k + E_p - \epsilon_{k-p}} - \frac{n_k(1-n_p)}{\epsilon_P + E_k - E_p - \epsilon_{k-p}}\right]. \tag{B10}$$

[1] C. L. Degen, F. Reinhard, and P. Cappellaro, Rev. Mod. Phys. **89**, 035002 (2017).

[2] R. Olf, F. Fang, G. E. Marti, A. MacRae, and D. M. Stamper-Kurn, Nat. Phys. **11**, 720 (2015).

[3] M. Hohmann, F. Kindermann, T. Lausch, D. Mayer, F. Schmidt, and A. Widera, Phys. Rev. A **93**, 043607 (2016).

[4] Q. Bouton, J. Nettersheim, D. Adam, F. Schmidt, D. Mayer, T. Lausch, E. Tiemann, and A. Widera, Phys. Rev. X **10**, 011018 (2020).

[5] D. Adam, Q. Bouton, J. Nettersheim, S. Burgardt, and A. Widera, arXiv:2105.03331.

[6] H. Edri, B. Raz, N. Matzliah, N. Davidson, and R. Ozeri, Phys. Rev. Lett. **124**, 163401 (2020).

[7] N. B. Jorgensen, L. Wacker, K. T. Skalmstang, M. M. Parish, J. Levinsen, R. S. Christensen, G. M. Bruun, and J. J. Arlt, Phys. Rev. Lett. **117**, 055302 (2016).

[8] M.-G. Hu, M. J. Van de Graaff, D. Kedar, J. P. Corson, E. A. Cornell, and D. S. Jin, Phys. Rev. Lett. **117**, 055301 (2016).

[9] L. A. Peña Ardila, N. B. Jørgensen, T. Pohl, S. Giorgini, G. M. Bruun, and J. J. Arlt, Phys. Rev. A **99**, 063607 (2019).

[10] Z. Z. Yan, Y. Ni, C. Robens, and M. W. Zwierlein, Science **368**, 190 (2020).

[11] A. Schirotzek, C.-H. Wu, A. Sommer, and M. W. Zwierlein, Phys. Rev. Lett. **102**, 230402 (2009).

[12] C. Kohstall, M. Zaccanti, M. Jag, A. Trenkwalder, P. Massignan, G. M. Bruun, F. Schreck, and R. Grimm, Nature (London) **485**, 615 (2012).

[13] M. Koschorreck, D. Pertot, E. Vogt, B. Frohlich, M. Feld, and M. Köhl, Nature (London) **485**, 619 (2012).

[14] F. Scazza, G. Valtolina, P. Massignan, A. Recati, A. Amico, A. Burchianti, C. Fort, M. Inguscio, M. Zaccanti, and G. Roati, Phys. Rev. Lett. **118**, 083602 (2017).

[15] I. Fritsche, C. Baroni, E. Dobler, E. Kirilov, B. Huang, R. Grimm, G. M. Bruun, and P. Massignan, Phys. Rev. A **103**, 053314 (2021).

[16] Y. Nishida, Phys. Rev. Lett. **114**, 115302 (2015).

[17] W. Yi and X. Cui, Phys. Rev. A **92**, 013620 (2015).

[18] M. Pierce, X. Leyronas, and F. Chevy, Phys. Rev. Lett. **123**, 080403 (2019).

[19] N. D. Mermin and H. Wagner, Phys. Rev. Lett. **17**, 1133 (1966).

[20] P. C. Hohenberg, Phys. Rev. **158**, 383 (1967).

[21] V. Berezinskiǐ, Sov. J. Exp. Theor. Phys. **34**, 610 (1972).

[22] J. M. Kosterlitz and D. J. Thouless, J. Phys. C **5**, L124 (1972).

[23] J. M. Kosterlitz and D. J. Thouless, J. Phys. C **6**, 1181 (1973).

[24] D. J. Bishop and J. D. Reppy, Phys. Rev. Lett. **40**, 1727 (1978).

[25] W. Dürr, M. Taborelli, O. Paul, R. Germar, W. Gudat, D. Pescia, and M. Landolt, Phys. Rev. Lett. **62**, 206 (1989).

[26] Z. Hadzibabic, P. Krüger, M. Cheneau, B. Battelier, and J. Dalibard, Nature (London) **441**, 1118 (2006).

[27] P. Cladé, C. Ryu, A. Ramanathan, K. Helmerson, and W. D. Phillips, Phys. Rev. Lett. **102**, 170401 (2009).

[28] S. Tung, G. Lamporesi, D. Lobser, L. Xia, and E. A. Cornell, Phys. Rev. Lett. **105**, 230408 (2010).

[29] C.-L. Hung, X. Zhang, N. Gemelke, and C. Chin, Nature (London) **470**, 236 (2011).

[30] R. Desbuquois, L. Chomaz, T. Yefsah, J. Léonard, J. Beugnon, C. Weitenberg, and J. Dalibard, Nat. Phys. **8**, 645 (2012).

[31] M. G. Ries, A. N. Wenz, G. Zürn, L. Bayha, I. Boettcher, D. Kedar, P. A. Murthy, M. Neidig, T. Lompe, and S. Jochim, Phys. Rev. Lett. **114**, 230401 (2015).

[32] P. A. Murthy, I. Boettcher, L. Bayha, M. Holzmann, D. Kedar, M. Neidig, M. G. Ries, A. N. Wenz, G. Zürn, and S. Jochim, Phys. Rev. Lett. **115**, 010401 (2015).

[33] L. Sobirey, N. Luick, M. Bohlen, H. Biss, H. Moritz, and T. Lompe, Science **372**, 844 (2021).

[34] D. R. Nelson and J. M. Kosterlitz, Phys. Rev. Lett. **39**, 1201 (1977).

[35] M. Randeria, J.-M. Duan, and L.-Y. Shieh, Phys. Rev. B **41**, 327 (1990).

[36] S. Zöllner, G. M. Bruun, and C. J. Pethick, Phys. Rev. A **83**, 021603 (2011).

[37] J. Kosterlitz, J. Phys. C **7**, 1046 (1974).

[38] E. Lifshitz and L. Pitaevskii, *Statistical Physics: Theory of the Condensed State*, Course of Theoretical Physics Vol. 9 (Elsevier Science, New York, 2013).

[39] E. Babaev and H. Kleinert, Phys. Rev. B **59**, 12083 (1999).

[40] S. S. Botelho and C. A. R. Sá de Melo, Phys. Rev. Lett. **96**, 040404 (2006).

[41] L. Salasnich, P. A. Marchetti, and F. Toigo, Phys. Rev. A **88**, 053612 (2013).

[42] D. S. Fisher and P. C. Hohenberg, Phys. Rev. B **37**, 4936 (1988).

[43] N. Prokof'ev, O. Ruebenacker, and B. Svistunov, Phys. Rev. Lett. **87**, 270402 (2001).

[44] P. Bloom, Phys. Rev. B **12**, 125 (1975).

[45] J. R. Engelbrecht and M. Randeria, Phys. Rev. B **45**, 12419 (1992).

[46] M. Bauer, M. M. Parish, and T. Enss, Phys. Rev. Lett. **112**, 135302 (2014).

[47] F. Marsiglio, P. Pieri, A. Perali, F. Palestini, and G. C. Strinati, Phys. Rev. B **91**, 054509 (2015).

[48] S. N. Klimin, J. Tempere, and J. T. Devreese, New J. Phys. **14**, 103044 (2012).

[49] R. Schmidt, T. Enss, V. Pietilä, and E. Demler, Phys. Rev. A **85**, 021602(R) (2012).

[50] A. J. Leggett, in *Modern Trends in the Theory of Condensed Matter* (Springer Berlin Heidelberg, 1980), pp. 13–27.

[51] M. J. H. Ku, A. T. Sommer, L. W. Cheuk, and M. W. Zwierlein, Science **335**, 563 (2012).

[52] H. Guo, Y. He, C.-C. Chien, and K. Levin, Phys. Rev. A **88**, 043644 (2013).

[53] H. Tajima, P. van Wyk, R. Hanai, D. Kagamihara, D. Inotani, M. Horikoshi, and Y. Ohashi, J. Low Temp. Phys. **187**, 677 (2017).

[54] H. Hu, B. C. Mulkerin, J. Wang, and X.-J. Liu, Phys. Rev. A **98**, 013626 (2018).

[55] H. Tajima and S. Uchino, New J. Phys. **20**, 073048 (2018).

[56] G. Bighin and L. Salasnich, Phys. Rev. B **93**, 014519 (2016).

[57] B. C. Mulkerin, L. He, P. Dyke, C. J. Vale, X.-J. Liu, and H. Hu, Phys. Rev. A **96**, 053608 (2017).

[58] A. Klein, M. Bruderer, S. R. Clark, and D. Jaksch, New J. Phys. **9**, 411 (2007).

[59] H. T. Ng and S. Bose, Phys. Rev. A **78**, 023610 (2008).

[60] M. Mehboudi, A. Sanpera, and L. A. Correa, J. Phys. A: Math. Theor. **52**, 303001 (2019).

[61] M. T. Mitchison, T. Fogarty, G. Guarnieri, S. Campbell, T. Busch, and J. Goold, Phys. Rev. Lett. **125**, 080402 (2020).

[62] F. Grusdt, N. Y. Yao, D. Abanin, M. Fleischhauer, and E. Demler, Nat. Commun. **7**, 11994 (2016).

[63] A. Camacho-Guardian, N. Goldman, P. Massignan, and G. M. Bruun, Phys. Rev. B **99**, 081105(R) (2019).

[64] A. Muñoz de las Heras, E. Macaluso, and I. Carusotto, Phys. Rev. X **10**, 041058 (2020).

[65] D. Pimenov, A. Camacho-Guardian, N. Goldman, P. Massignan, G. M. Bruun, and M. Goldstein, Phys. Rev. B **103**, 245106 (2021).

[66] N. Baldelli, B. Juliá-Díaz, U. Bhattacharya, M. Lewenstein, and T. Graß, Phys. Rev. B **104**, 035133 (2021).